TSINGHUA SCIENCE AND TECHNOLOGY
ISSN 1007-0214 22/24 pp1695-1697
Volume 4, Number 4, December 1999

Observation of the Metallic Vapor from a Plasma Focus*

WANG Xinxin (王新新), YANG Jinji (杨津基)

Department of Electrical Engineering, Tsinghua University, Beijing 100084

Abstract Although many scientists suggested that the ionized metallic vapor produced in plasma focus plays a significant role in the X-ray emission, they did not give a visual image of the metallic vapor. In this paper the evolution of plasma sheath above the anode was recorded with a laser differential interferometer and the metallic vapor produced on the target surface by bombardment of an intense electron beam was observed for the first time. The results can help understanding of the physical process of the X-ray emission from plasma focus.

Key words plasma focus; X-ray emission; interferogram

Introduction

Dense plasma focus devices (DPF)[1] are used to produce pulsed plasmas with high temperatures (10^7 K) and densities (10^{19} – 10^{20} cm^{-3}) by means of extremely large pulsed electrical discharge in gases. A Mather type DPF is shown in Fig. 1. When the spark gap is triggered, the high voltage from the charged condenser bank is applied to the coaxial electrodes (anode and cathode). Breakdown occurs along the cylindrical insulator, forming an azimuthally symmetric plasma sheath (PS). By the Lorentz force action the conducting PS moves upwards along the coaxial electrodes. When the PS arrives at the top of the anode, it rapidly compresses towards the axis of the anode and forms a plasma column (plasma focus). Due to micro-instabilities the pinched plasma column collapses and leads to the generation of powerful beams of electrons, ions, X-rays, and neutrons when the filling gas is deuterium. It has been found that the emission phenomena in plasma focus are strongly related to the processes above the anode[2]. Although it was believed by many scientists that the ionized metallic vapor is produced in the plasma focus and plays a significant role in the X-ray emission[3,4], they were unable to give a visual image of the metallic vapor. In this paper the metallic vapor from the target of anode was observed for the first time.

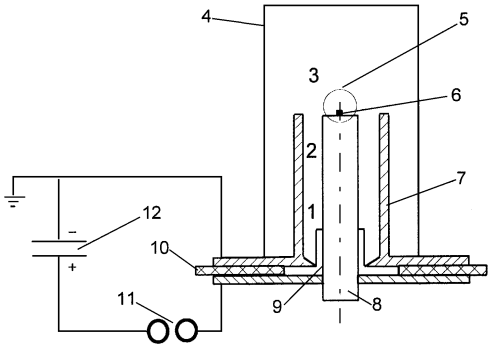

Fig. 1 Plasma focus device of Mather type
1, plasma sheath in breakdown phase; 2, plasma sheath in rundown phase; 3, plasma sheath in pinch phase; 4, vacuum chamber; 5, observation window; 6, target on anode; 7, cathode; 8, anode; 9, insulator; 10, insulating plate; 11, spark gap; 12, capacitor

1 Experiment and Results

The experiments were performed using DPF-16 (16 kJ, 20 kV, 380 kA)[2]. The electrode geometry represents an accelerator of Mather type. Both anode (66 mm diam.) and cathode are 265 mm in length and were machined from oxygen-free copper. The anode is a solid cylinder with a tungsten stud, 10 mm in diameter and 6 mm high, set on the top as a target for electron bombardment. The

Received: 1998-05-27; revised: 1999-04-25
* Supported by the National Natural Science Foundation of China (No. 59207068)

working gas is hydrogen with a pressure of 70- 650 Pa. The evolution of the PS above the anode was recorded with a laser differential interferometer[5].

Figure 2 is the typical interferograms taken at 200 Pa filling pressure in the region that shows a field of view about 60 mm in diameter (corresponding to the observation window, i.e., the circle in Fig. 1).

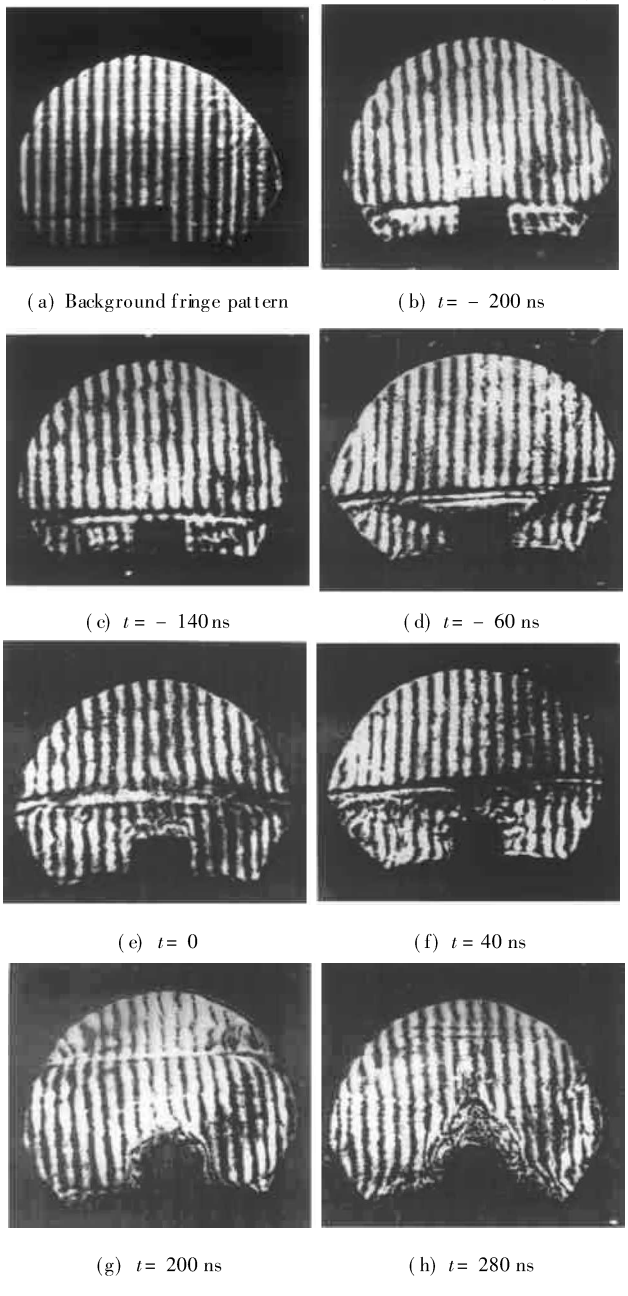

(a) Background fringe pattern (b) t= - 200 ns

(c) t= - 140 ns (d) t= - 60 ns

(e) t= 0 (f) t= 40 ns

(g) t= 200 ns (h) t= 280 ns

Fig. 2 The interferograms of PS evolution above the target of anode taken at hydrogen pressure of 200 Pa

Figure 2(a) is the background fringe pattern, i.e., undisturbed fringe without plasma. At the bottom of the picture the target as well as the top end of anode can be clearly seen. As the target is 10 mm in diameter and 6 mm high, it was used as a dimension scale for quantitative measurement. The time reference t = 0 was set at the pinch spike in the dI/dt waveform, which corresponds to the instant of maximum compression of plasma above the anode. So the pictures taken at t < 0 correspond to the PS compression towards the axis of anode, t = 0 to the PS forming a plasma column with a minimal radius and t > 0 to the pinched plasma column collapsing and then expanding.

From Figs. 2(b), 2(c), and 2(d) taken at t < 0, we can see a loudspeaker-like PS moving upwards and inwards, which indicates the PS compression. In Fig. 2(e) taken at t = 0, the PS has compressed into a plasma column with a minimal radius and takes the T shape. In the Fig. 2(f) taken at t = 40 ns we can see the pinched plasma column beginning to expand due to its collapse. Since Fig. 2(g) is taken at the time long after the pinched plasma column collapsed and the PS is expanding, the horizontal line consisting of the disturbed fringes moves up and the fringes right above the target become undisturbed again. In this case it is usually considered that the focus is over. But in Fig. 2(h), taken 80 ns later, we can see that a small volume of high density emerges from the target of anode, while the PS has moved out of the view field and disappeared.

We believe the high density volume to be the metallic vapor produced on the target surface by bombardment of an intense electron beam which originated from the collapsing pinch as usually considered. This view is supported by the facts given below. First, the erosion of the target after many shots of discharge confirms the evaporation of the target material. Secondly, the high density volume can not be seen when the solid anode with a target is replaced by a hollow anode[6]. Thirdly, since the high density volume appears well after the focus was over, it must be something new other than the PS. Finally, the delay time from the pinched plasma column to the appearance of the high density volume was about 280 ns, which may be the time required to produce a sufficient concentration of metallic vapor to be seen clearly in the interferogram. It is important to notice that this delay time is very consistent with the results obtained by Harries[3]. He found that the main hard X-ray emission occurred several hundred nanoseconds after the focus was over and he thought it seemed to be from a metallic plasma released from the anode surface by bombardment of an intense electron beam.

Figures 3(a) and 3(b) are two interferograms, taken at 220 ns and 300 ns respectively when the filling pressure of hydrogen is 330 Pa, which shows the development of the metallic vapor more clearly.

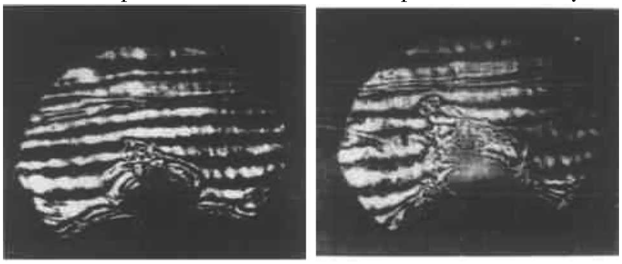

(a) $t = 220$ ns (b) $t = 300$ ns

Fig. 3 Interferograms showing the developing of the metallic vapor taken at hydrogen pressure of 330 Pa

2 Conclusions

The evolution of the plasma sheath above the anode of DPF-16 is recorded with a laser differential interferometer and the metallic vapor produced on the target surface by bombardment of an intense electron beam was observed for the first time. The observation will help understanding of the physical process of the X-ray emission from plasma focus.

References

1 Mather J W. Methods of Experimental Physics. Vol. 9B. Academic Press, New York, 1971
2 Wang Xinxin, Yang Jinji. Effect of plasma sheath structure in plasma focus. IEEE Trans on Plasma Science, 1993, 21(1): 175- 180
3 Harries W L, Lee J H, McFarland D R. Space and time resolved emission of hard X-rays from a plasma focus. Plasma Physics, 1978, 20: 963 - 969
4 Wang Jia, Yang Jinji. A study of X-ray emission from the anode region in a plasma focus device. J Phys D: Appl Phys, 1988, 21: 700 - 709
5 Wang Xinxin, Yang Jinji, Han Min. Application of a laser differential interferometer to plasma focus. Plasma Sources Science & Technol, 1993, 2: 153- 157
6 Lu Minfang. Use of a double-wollaston prism laser differential interferometer in a plasma focus. Rev Sci Instrum, 1997, 68(2): 1149 - 1153

(continued from page 1691)

3 Conclusions

The full-function numerical method for flow over a self-excited vibrating body over flow is presented in this paper. It consists of calculation of 3-D viscous flow, determination of unsteady aerodynamic work and damping work, determination of the equilibrium amplitude and the dynamic stress as well as life evaluation. This is a systematic method for safety analysis, better and suitable for applications. The feasibility of this numerical method is also demonstrated by the calculated example of a steam turbine blading.

References

1 • ;1995, 16(3): 305 - 308
Chen Zuoyi, Wang Ruoshui. Determine 3-D viscous stall flow in turbomachinery using parametric polynomial method. Journal of Engineering Thermophysics, 1995, 16(3): 305 - 308
2 • ;952004. • • ;1995. II- 88- 95
Chen Zuoyi. Determine 3-D vicious oscillating flow in Turbomachinery using parametric polynomial method. In: Conference of Engineering Thermophysics. 952004. Beijing, 1995. II- 88-92
3 • ;1988
Chen Zuoyi, Jiang Zikang, Sun Xijiu. Oscillating Fluid Mechanics. Hydroelectric Press, Beijing, 1988
4 • • • • • • • • • • • • • • • • • • • ;1988
Xu Hao. Fatigue Strength. Higher Education Press, Beijing, 1988
5 • ;1991
Cao Chunhua, Zou Shijian. Strength Analysis Method and Its Application. National Defense Industry Press, Beijing, 1991